British Journal of Pharmacology (1998) 125, 209–217 © 1998 Stockton Press All rights reserved 0007–1188/98 $12.00
http://www.stockton-press.co.uk/bjp

Molecular cloning and functional characterization of a rat somatostatin $sst_{2(b)}$ receptor splice variant

[1,2]Marcus Schindler, [1]Emma J. Kidd, [1]Alan M. Carruthers, [1]Mark A. Wyatt, [1]Emma M. Jarvie, [1]Lynda A. Sellers, [1]Wasyl Feniuk & [1]Patrick P.A. Humphrey

[1]Glaxo Institute of Applied Pharmacology, Department of Pharmacology, University of Cambridge, Cambridge, CB2 1QJ

1 The mouse somatostatin (SRIF) sst_2 receptor exists in two splice variants, $sst_{2(a)}$ and $sst_{2(b)}$, which differ in their intracellular carboxy-termini only. The murine $sst_{2(b)}$ receptor was reported to be less prone to agonist-induced desensitization as compared with the $sst_{2(a)}$ receptor. To determine whether a $sst_{2(b)}$ splice variant with similar functional characteristics exists in the rat, we have isolated a cDNA fragment from rat gastric mucosa encoding a $sst_{2(b)}$ receptor and expressed the full-length protein in CHO-K1 cells for functional characterization.

2 This study provides the first evidence for the occurrence in the rat of the $sst_{2(b)}$ receptor, which has a 15 amino acid carboxy-terminus differing in composition to the 38 amino acid C-terminus of the rat $sst_{2(a)}$ receptor.

3 In CHO-K1 cells expressing rat recombinant $sst_{2(a)}$ or $sst_{2(b)}$ receptors, SRIF caused concentration-dependent increases in extracellular acidification rates (EAR) with pEC_{50} values of 9.0 and 9.9, respectively. Pre-treatment with pertussis toxin (Ptx) caused a rightward displacement of the SRIF concentration-effect curves with pEC_{50} values of 8.3 ($sst_{2(a)}$) and 8.4 ($sst_{2(b)}$).

4 SRIF (3 pM – 3 nM) also caused concentration-dependent inhibition of forskolin-stimulated cyclic AMP formation in CHO-$sst_{2(a)}$ cells (pIC_{50} 10.5) and CHO-$sst_{2(b)}$ cells (pIC_{50} 10.4). The degree of inhibition was less with higher concentrations of SRIF resulting in bell-shaped concentration-effect curves. Following pre-treatment with Ptx, the inhibitory effect of SRIF was abolished and SRIF caused only increases in cyclic AMP formation.

5 Both the SRIF-induced increases in EAR and inhibition of cyclic AMP formation were susceptible to agonist-induced desensitization, but this was less apparent following pre-treatment with Ptx.

6 This demonstrates that the operational characteristics of the recombinant rat $sst_{2(a)}$ and $sst_{2(b)}$ receptors are broadly similar. Both isoforms couple to Ptx-sensitive as well as -insensitive G proteins and are equally prone to agonist-induced desensitization.

Keywords: Cloning; RT-PCR; somatostatin receptors; splice variants; microphysiometry; adenylate cyclase; $sst_{2(a)}$, $sst_{2(b)}$

Introduction

Somatostatin (SRIF) mediates its many physiological actions through binding to membrane-bound receptors (see Epelbaum, 1986 for review). Recently, at least five genes encoding high affinity somatostatin receptors have been cloned, which are now termed sst_1-sst_5 (Hoyer *et al*., 1995). These somatostatin receptors couple to heterotrimeric guanine nucleotide-binding (G) proteins and belong to the class of seven helical transmembrane domain receptors (reviewed by Reisine & Bell, 1995).

The distribution of the mRNA for these receptors has been extensively studied in the rat central nervous system and, to a lesser degree, in the gastrointestinal tract (see Schindler *et al*., 1996, for review). With the advent of selective antibodies, the distribution of the rat $sst_{2(a)}$ receptor protein has been mapped in the rat central nervous system, spinal cord and periphery (Dornaud *et al*., 1996; Hunyady *et al*., 1997; Schindler *et al*., 1997), where it shows a widespread distribution.

The murine sst_2 receptor is the only SRIF receptor reported to exist as two splice variants termed $sst_{2(a)}$ and $sst_{2(b)}$. The mouse splice variant $sst_{2(b)}$ which was cloned by Vanetti and colleagues, only differs from the $sst_{2(a)}$ receptor in the composition of the intracellular carboxy-terminus (Vanetti *et al*., 1992) and is 23 amino acids shorter than the $sst_{2(a)}$ receptor.

In situ hybridization studies to detect $sst_{2(a)}$ and $sst_{2(b)}$ mRNAs indicate an overlapping distribution of the mRNAs for both splice variants in the mouse central nervous system (Vanetti *et al*., 1994), but no data are available concerning the distribution of the $sst_{2(b)}$ receptor protein in either the central nervous system or peripheral tissue. Functionally, the two isoforms have been claimed to differ in their coupling to adenylate cyclase in that the mouse $sst_{2(a)}$ receptor did not effectively couple to adenylate cyclase. Furthermore, the mouse $sst_{2(b)}$ receptor was reported to be less prone to agonist-induced desensitization as compared to the mouse $sst_{2(a)}$ receptor (Reisine *et al*., 1993; Vanetti *et al*., 1993).

It has previously been shown in functional studies that the somatostatin receptor involved in the inhibition of gastric acid secretion in rat isolated gastric mucosa resembles the recombinant sst_2 receptor and is resistant to agonist-induced desensitization (Lloyd *et al*., 1995; Wyatt *et al*., 1996). We attempted to identify the sst_2 receptor in the rat stomach with a view to determining whether the $sst_{2(b)}$ splice variant, identified in the mouse (Vanetti *et al*., 1992), also exists in the rat as previously suggested (Patel *et al*., 1993; Wyatt *et al*., 1996). Furthermore, following the cloning and stable expression of a rat $sst_{2(b)}$ receptor described here, the operational properties of the recombinant $sst_{2(b)}$ receptor expressed in Chinese hamster ovary (CHO) K1 cells were compared to those of the rat $sst_{2(a)}$ receptor.

[2] Author for correspondence.

A preliminary account of these findings has been presented to the British Pharmacological Society (Kidd *et al*., 1998; Schindler *et al*., 1998).

Methods

Molecular cloning

Rat gastric mucosa was isolated as described (Wyatt *et al*., 1996) and total RNA was extracted according to a method described previously (Chomczynski & Sacchi, 1987), but incorporating an initial purification step through a 5.7 M caesium chloride gradient according to Sambrook *et al*. (1989). Poly(A)$^+$ RNA was purified on an oligo(dT)-cellulose column (mRNA Separator Kit, Clontech) and treated with RNase-free DNase I (Stratagene) for 30 min at 37°C. First-strand cDNA was synthesized from 2 μg of poly(A$^+$) RNA using an oligo(dT)$_{18}$ primer and Moloney-murine leukaemia virus reverse transcriptase (Advantage RT-for-PCR Kit, Clontech). Control reactions in the absence of reverse transcriptase (RT) were also carried out. Somatostatin sst_2 receptor-specific primers were designed as follows based on the sst_2 receptor DNA sequence from Kluxen *et al*. (1992): forward 5′-GCATGGTACACGGGTTTCATTA-3′ (primer 1, nucleotides 974–995); reverse 5′-CCGCTATGTAATCTCGTGATC-3′ (untranslated 3′ region, nucleotides 1801–1821, primer 2). For the amplification of β-actin mRNA the following primers were used: 5′-GAGAGGCATCCTGACCCTGA-3′ (forward) and 5′-TAGTGTTACGGTCACCCATGCPCR-3′ (reverse) amplifying a 276 bp DNA fragment. Polymerase chain reaction (PCR) was performed using 2 μl of the first-strand reaction as a template. Amplifications were performed with *Taq* DNA polymerase (2.5 U, Promega) using 1 μM of each of the primers and 200 μM of each of the deoxy nucleotide triphosphates (dNTP). The conditions were as follows: 95°C, 35 s; 60°C, 45 s; 72°C, 45 s; 40 cycles and a final extension at 72°C, 10 min. The resulting PCR products were analysed by agarose gel electrophoresis, bands with the correct size were excised from the gel, purified using GeneClean (Bio101) and cloned into pCR II vector (Original TA Cloning Kit, Invitrogen) according to the manufacturer's instructions. Plasmid DNA was manually sequenced (Sanger *et al*., 1977) using the Sequenase v2.0 enzyme (Amersham).

Expression

To construct a full-length, hemagluttinin (HA) epitope-tagged $sst_{2(b)}$ receptor DNA, a *Bam*HI/*Not*I fragment encoding the putative rat $sst_{2(b)}$ receptor was isolated from the plasmid vector pCRII carrying the $sst_{2(b)}$ PCR DNA (see above). This fragment was used to replace the $sst_{2(a)}$ receptor carboxy-terminus in *palphaCA12* (Affymax) which had been cut out using a *Bam*HI/*Not*I double digest (see Figure 3 for a schematic view of the cloning strategy). The epitope tag is located two amino acids from the amino-terminus of the receptor protein (Figure 3). Correct in-frame insertion of this fragment was confirmed by double-stranded DNA sequencing of positive clones. The expression vector containing the coding region (357 amino acids including the epitope tag) of the rat $sst_{2(b)}$ receptor was transfected into CHO-K1 cells using Lipofectamine (Life Technologies) as recommended by the manufacturer. Stable cell lines were created using selection with G418 (500 μg ml^{-1}). Subsequent single cell dilution cloning yielded a number of clonal cell lines, which were screened for somatostatin receptor expression by receptor ligand binding using [^{125}I]-[Tyr^{11}]-SRIF. The clone with the highest expression level was used for further analysis.

Cell culture and immunocytochemistry

Cell culture and immunocytochemistry on CHO-K1 cells using the anti-HA antibody (Boehringer Mannheim, monoclonal antibody clone 12CA5; concentration 5 μg ml^{-1}) was carried out as described previously (Schindler *et al*., 1997). Primary antibody was detected using cyanine-3 (Cy3)-conjugated sheep anti-mouse IgG antibody (Sigma) at a 1 : 200 dilution, washing in phosphate buffered saline (PBS) and water, followed by mounting coverslips in Fluoromount (DAKO). Cells were viewed using a Nikon Optiphot-2 microscope.

Pertussis toxin (Ptx, SIGMA) pre-treatment was carried out for 18–24 h before the experiment at a concentration of 100 ng ml^{-1} of culture media.

Membrane preparations and receptor ligand binding

Cell membrane preparations for receptor binding studies and radioligand binding assays were performed as described previously (Castro *et al*., 1996). To calculate Kd and B_{max} values from competition studies, the following equations were used: $Kd = IC_{50} - [A]$, where Kd is the dissociation equilibrium constant of the radioligand, IC_{50} is the half-maximal inhibitory concentration of SRIF-14 and [A] is the concentration of [^{125}I]-[Tyr^{11}]-SRIF present; $B_{max} = ([B] \times (IC_{50})/[A]$, where B_{max} is the receptor density and [B] is the concentration of specific [^{125}I]-[Tyr^{11}]-SRIF bound to the receptor in the absence of competing ligand.

Microphysiometry

Somatostatin- (SRIF)-induced increases in extracellular acidification rates (EAR) were measured by microphysiometry using the Cytosensor® (Molecular Devices, U.S.A.) as previously described (Castro *et al*., 1996). In brief, cells were seeded into Cytosensor® cups (Costar, U.K.) at a density of 400,000 cells per well 24 h prior to the experiment. Cells were perfused with bicarbonate-free DMEM (pH 7.4) containing 1 mg ml^{-1} bovine serum albumin (BSA) at a rate of about 120 μl min^{-1}. The rate of extracellular acidification was measured over a 30 s period. Drugs were added for a period of 3 min 10 s, followed by washing in media (30–90 min) before applications of subsequent drug concentrations. All cells were initially challenged with a single concentration (3 μM) of UTP which was used as an internal standard.

Adenylate cyclase assay

CHO-K1 cells expressing rat $sst_{2(a)}$ or $sst_{2(b)}$ receptors were suspended in serum-free DMEM/Ham's F-12 nutrient (1 : 1) mix, supplemented with bacitracin (0.2 mg ml^{-1}) and 3-isobutyl-l-methylxanthine (IBMX; 0.5 mg ml^{-1}) and pre-warmed to 37°C for 15 min. Measurements of cyclic AMP were performed in triplicate on 170,000 cells (assay volume 300 μl) in the presence of forskolin (10 μM) for 10 min at 37°C. Reactions were terminated by the addition of 10 μl 10 M HCl, followed by neutralization with 10 μl 10 M NaCl and 200 μl 1 M Tris-HCl (pH 7.0). Samples were centrifuged at 8800 $\times$ *g* for 20 min. Fifty microlitres of supernatant were added to 100 μl [^{3}H]-cyclic AMP (approximately 1 nM; specific activity, 41 Ci mmol^{-1}, Amersham International) in 50 mM Tris-HCl, 100 mM NaCl, 5 mM di-sodium ethylenediamine tetraacetate, pH 7.0 and binding to the cyclic AMP-binding portion of

protein kinase A (100 μl in the above buffer; approximately 2 μg per tube) was measured after 2–4 h at 4°C according to the method of Brown *et al*., (1971). Binding reactions were terminated by rapid vacuum filtration onto pre-wetted (0.5% w/v PEI) GF/B filters and bound radioactivity determined by liquid scintillation spectrometry. In desensitization studies, cultures were pre-incubated with SRIF (10 nM) in serum-free DMEM/Ham's F-12 media for 1 h at 37°C. Cell monolayers were then extensively washed (20×25 ml per 225 cm^2 culture flask) in the above media and harvested cells were placed on ice prior to experimentation. Adenylate cyclase activity was measured in the presence of 10 μM forskolin and responses to SRIF were expressed as a percentage of forskolin-stimulated activity. Maximal inhibition of cyclic AMP accumulation was taken as the lowest cyclic AMP concentration measured on each individual experiment and higher agonist concentrations were excluded from the analysis when calculating a pIC_{50} for the inhibition of cyclic AMP accumulation. The pIC_{50} values for decreasing cyclic AMP accumulation were calculated as the negative $\log_{10}$ of the molar concentration of the agonist producing 50% of the maximal response. Where possible, pEC_{50} values were calculated for the stimulatory effect of SRIF following Ptx pre-treatment. Basal and forskolin stimulated values were measured as nmoles per 170,000 cells.

Statistical analysis

All IC_{50} and EC_{50} values are geometric means (95% confidence limits) of n observations. All other values are arithmetic means $\pm$ s.e.means. Tests for statistically significant differences were carried out using a two-tailed unpaired Student's t-test.

Materials

All chemicals were obtained from Sigma U.K. unless otherwise stated. Somatostatin was obtained from Peninsula Laboratories Europe Ltd. (St Helens, Merseyside, U.K.). Dulbecco's modified Eagle's medium (DMEM)/Ham's F12 nutrient, M199 foetal calf serum (FCS), Glutamax I and G418 sulphate were obtained from Life Technologies (Paisley, U.K.). Restriction enzymes were obtained from New England Biolabs. CHO-K1 cells expressing the hemagglutinin epitope-tagged version of the rat $sst_{2(a)}$ receptor, as well as the rat $sst_{2(a)}$ receptor cDNA construct, were provided by Affymax (Palo Alto, California, U.S.A.).

Results

Molecular cloning and expression

After isolation of RNA from rat gastric mucosa, RT-PCR was carried out using oligonucleotide primers that would potentially allow differentiation between the 'long' ($sst_{2(a)}$) and the 'short' ($sst_{2(b)}$) splice variants of the somatostatin sst_2 receptor as proposed by Patel *et al*. (1993); (Figure 1). Following gel electrophoresis on an ethidium bromide containing agarose-gel, two significant cDNA bands were observed (Figure 1). The bands were excised from the gel and sub-cloned into the pCR II vector (Invitrogen). The DNA sequence of the largest band (848 base pairs) was found to be identical to the previously cloned $sst_{2(a)}$ receptor (Kluxen *et al*., 1992, data not shown) while the smaller (527 bp) band contained a novel sequence of the rat $sst_{2(b)}$ receptor. A weak intermediate band was obtained in addition which had no sequence identity with any known somatostatin receptor sequence (data not shown). The deduced amino acid sequence of the putative carboxy-terminus of rat $sst_{2(b)}$ (15 amino acids) had 73% homology with the previously published sequence of the mouse $sst_{2(b)}$ receptor (Vanetti *et al*.,

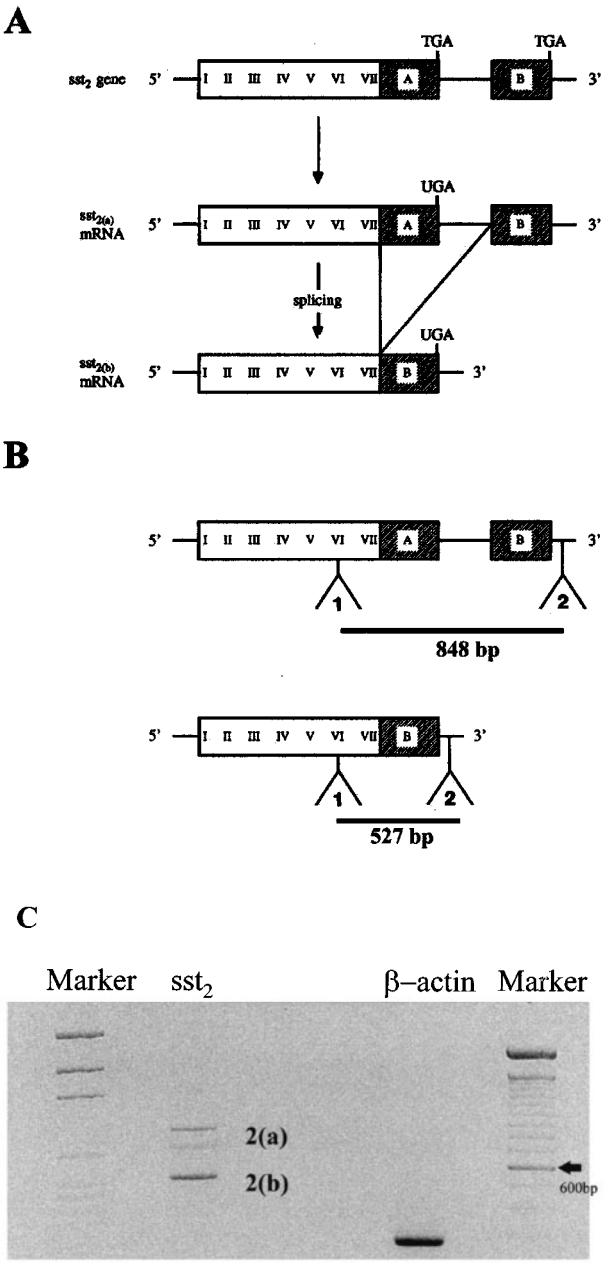

Figure 1 (A) Differential splicing of the sst_2 gene results in the generation of two mRNA species, coding for $sst_{2(a)}$ and $sst_{2(b)}$ receptors, respectively, which differ in the length and composition of their carboxy termini (shaded boxes) only. (B) Strategy used to isolate a $sst_{2(b)}$ receptor splice variant. Shown are the oligonucleotide primers 1 and 2 (see Materials) and their locations on the sst_2 gene sequence. PCR products with two different molecular weights will be amplified. (C) Agarose gel of PCR products obtained from a reverse transcription PCR reaction from rat gastric mucosa, using the primer pair described above (lane sst_2). Two significant cDNA bands were observed, the DNA sequence of largest band (848 base pairs) was found to be identical to the previously cloned $sst_{2(a)}$ receptor while the smaller (527 bp) contained the novel rat $sst_{2(b)}$ receptor sequence. The intermediate band was found not to be related to any known somatostatin receptor sequence. As a quality control to demonstrate the integrity of the RNA β-actin primers were used to amplify a 276 bp fragment (lane β-actin). Marker bands shown on the right are from the 1 kb ladder (Life Technologies) and on the left from Lambda *Hind*III (New England Biolabs).

1992, Figure 2). Comparison of this novel DNA sequence with the overlapping regions of the sst_2 receptor DNA (Kluxen *et al*., 1992) showed the sequences to be identical apart from an additional guanosine residue in our sequence, located in the 3′ untranslated region (Figure 2). The sequence of the rat $sst_{2(b)}$ receptor fragment has been deposited in the EMBL sequence database (Accession number X98234). To determine whether the cloned $sst_{2(b)}$ fragment encoded a functional receptor protein, a full length, HA-epitope-tagged $sst_{2(b)}$ cDNA was constructed, encoding 357 amino acids. The rat $sst_{2(b)}$ receptor was stably expressed in CHO-K1 cells.

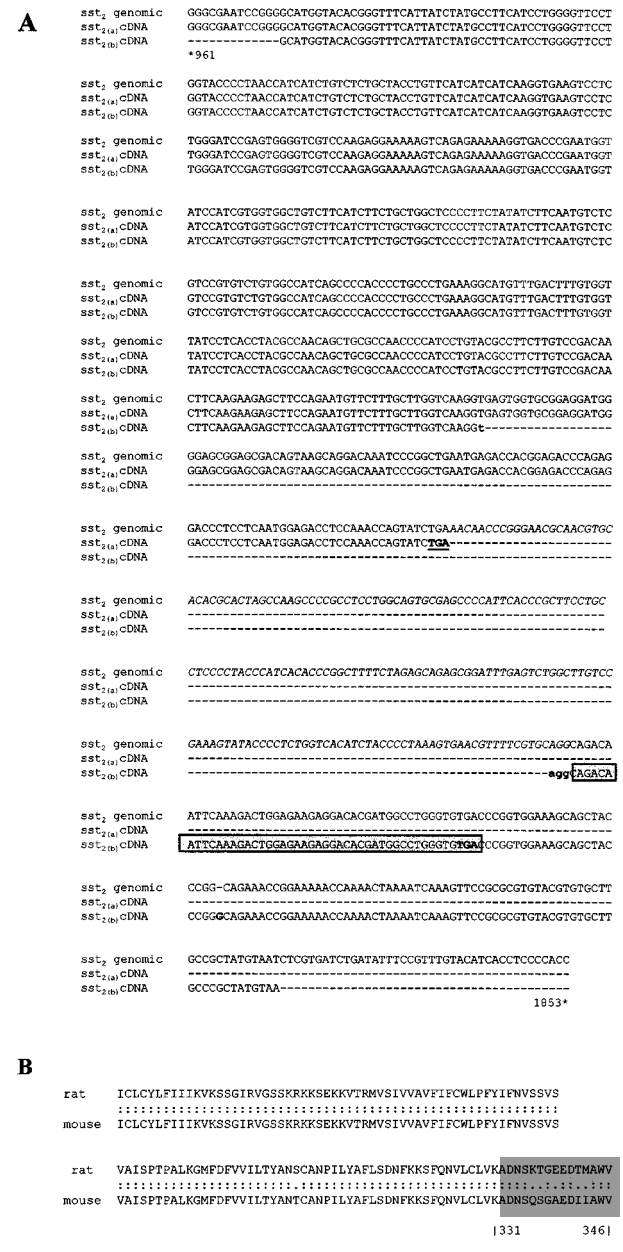

Figure 2 (A) Comparison of the sequence obtained after sub-cloning the 527 bp PCR fragment (rat $sst2_{(b)}$) and its comparison to the rat $sst_{2(a)}$ receptor gene. Underlined are the stop codons. In small bold script, the putative splice donor/acceptor sites are shown. Note the additional guanosine residue in the untranslated region shown in bold script. Boxed is the cDNA sequence encoding the putative carboxy-terminal stretch (15 amino acids) of the $sst_{2(b)}$ receptor. (B) Comparison of the carboxy-terminal end of the rat $sst_{2(b)}$ to that of the mouse $sst_{2(b)}$ receptor. Boxed is the amino acid stretch that differs significantly between the two species. Numbers correspond to amino acids in the mouse $sst_{2(b)}$ receptor sequence.

Localization of the receptor protein in CHO-K1 cells

The epitope-tagged $sst_{2(b)}$ receptor (Figure 3A) expressed in CHO-K1 cells was detected using immunocytochemistry. The anti-HA antibody specifically labelled the receptor protein on the cytoplasmic membrane, with a number of immunoreactive granules which appeared as punctate staining over the cytoplasm (Figure 3B).

Receptor binding

Radioligand binding studies on membranes prepared from CHO-K1 cells stably expressing the somatostatin $sst_{2(a)}$ and $sst_{2(b)}$ receptor, respectively, were carried out as described previously (Castro *et al*., 1996). SRIF caused a concentration-dependent inhibition of specific [^{125}I]-[Tyr^{11}]-SRIF binding in membranes prepared from CHO-$sst_{2(a)}$ ($pIC_{50} = 10.3 \pm 0.12$; $n = 3$) and CHO-$sst_{2(b)}$ ($pIC_{50} = 10.2 \pm 0.10$; $n = 3$) cells. The estimated B_{max} values in both clonal cell lines were similar, 10.3 ± 1.0 ($sst_{2(a)}$) and 7.3 ± 1.6 ($sst_{2(b)}$) pmole/mg protein, respectively ($n = 3$, for both data sets). No specific binding was detected in untransfected CHO-K1 cells (data not shown).

Microphysiometry

In both CHO-$sst_{2(a)}$ and CHO-$sst_{2(b)}$ cell lines, the basal rates of EAR were 100–300 μV/s (0.1–0.3 pH unit min^{-1}). A single challenge of UTP (3 μM) was used as an internal control to demonstrate viability of the cells. SRIF caused concentration-dependent increases in EAR in CHO-K1 cells expressing either rat $sst_{2(a)}$ or $sst_{2(b)}$ receptors [pEC_{50} values: 9.0 ± 0.2 ($n = 4$) and 9.9 ± 0.1 ($n = 6$); maximal increase: 180 ± 14 and 161 ± 8 μV/s respectively] (Figure 4). Ptx pre-treatment caused a rightward displacement of the SRIF concentration-effect curves [pEC50 values: 8.3 ± 0.2 ($n = 3$) and 8.4 ± 0.2 ($n = 5$); maximal increase: 155 ± 17 and 109 ± 10 μV/s, respectively] (Figure 4). UTP-induced increases in EAR in Ptx-treated cells did not significantly differ from those of untreated cells [$sst_{2(a)}$ 119.2 ± 15.1 ($n = 10$); $sst_{2(a)}$ Ptx 127.4 ± 10.8 ($n = 8$); $sst_{2(b)}$ 188.4 ± 14.1 ($n = 9$); $sst_{2(b)}$ Ptx 173.3 ± 20.6 ($n = 8$), all values in μV/s].

In some experiments, it became apparent that the sequential non-cumulative application of maximal and supramaximal concentrations of SRIF to both CHO-$sst_{2(a)}$ and CHO-$sst_{2(b)}$ cell lines, even at 60–90 min intervals, caused a loss of reactivity, which was manifested by reduced peak height and duration of the EAR increases. This is shown for CHO-$sst_{2(b)}$ cells in Figure 5A. Over a similar agonist concentration range, Ptx-treated CHO-$sst_{2(b)}$ cells exhibited a concentration-dependent increase in EAR and did not show similar desensitization following agonist-treatment (Figure 5A). To investigate any differential desensitization further, two maximal concentrations (1 μM) of SRIF were given with an intervening 60 min interval (Figure 5B) and the EAR increases caused by the first SRIF challenge were set as 100%. EAR response to the second SRIF challenge were significantly smaller (Student's unpaired *t*-test, $P \leqslant 0.005$) in CHO-$sst_{2(a)}$ cells (untreated 53 $\pm$3%, Ptx-treated 77 ± 3%), as well as in $sst_{2(b)}$ cells (untreated 35 ± 4%; Ptx-treated 83 ± 1%).

Adenylate cyclase

Receptor coupling to adenylate cyclase was assessed in CHO-K1 cells stably expressing $sst_{2(a)}$ and $sst_{2(b)}$ receptors. Basal levels of cyclic AMP were $0.13 \pm$ 0.01 nmoles ($n = 4$) and 0.18 ± 0.02 nmoles cyclic AMP ($n = 6$) for CHO-$sst_{2(a)}$ and

CHO-$sst_{2(b)}$, respectively. Following Ptx pretreatment (100 ng ml^{-1}; 22–24 h), the respective basal values were 0.61 ± 0.09 nmoles ($n=3$) and 0.38 ± 0.01 nmoles ($n=4$). Although incubation with forskolin (10 μM) for 10 min caused a variable (20 to 100 fold) increase in cyclic AMP accumulation, the percentage of inhibition of adenylate cyclase by SRIF did not vary as a function of the degree of stimulation achieved by forskolin.

In CHO-$sst_{2(a)}$ cells, SRIF (3 pM-3 nM) potently decreased forskolin-stimulated cyclic AMP levels by $96.6 \pm 3.9\%$ (pIC_{50}: 10.5 ± 0.10; $n=4$). However, above 10 nM SRIF, increasing concentrations of SRIF caused a smaller degree of inhibition, resulting in bell-shaped concentration-effect curves (Figure 6A). In $sst_{2(b)}$-expressing cells, SRIF also inhibited forskolin-stimulated adenylate cyclase activity with similar potency to that in CHO-$sst_{2(a)}$ cells (pIC_{50}: 10.4 ± 0.22; $n=6$) although the

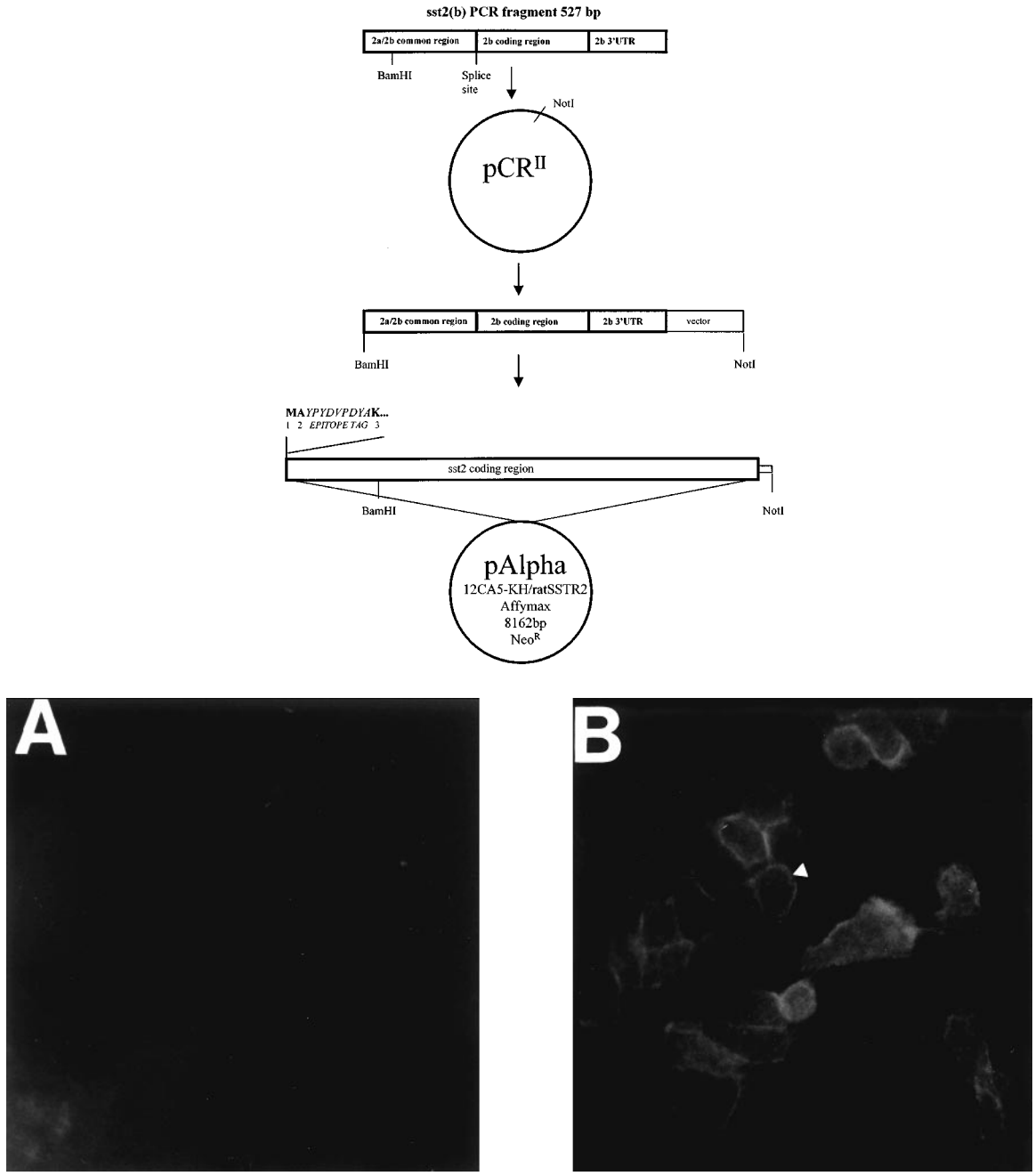

Figure 3 Cloning strategy and expression of the epitope-tagged $sst_{2(b)}$ receptor. Upper panel: To construct a full-length $sst_{2(b)}$ receptor for expression, the PCR fragments generated (Figure 2), containing the $sst_{2(b)}$ receptor coding sequence, the splice site, a 5′ common region and a 3′ untranslated region (UTR) were cloned into the vector pCR^{II} (Invitrogen). From this, a *Bam*HI/*Not*I fragment was isolated. This was used to replace a *Bam*HI/*Not*I fragment of the pAlpha (Affymax)-$sst_{2(a)}$ receptor construct, which contained the coding region of the $sst_{2(a)}$ receptor carboxy-terminus. The resulting construct contained an epitope-tagged 5′ region which is identical in both $sst_{2(a)}$ and $sst_{2(b)}$ receptors plus the entire coding region and the 3′UTR of the rat $sst_{2(b)}$ receptor. Amino acid abbreviations (single letter code) shown correspond to the first three amino acids of the rat $sst_{2(a/b)}$ receptor (numbers 1–3). The hemagluttinin epitope tag comprises nine amino acids which are shown in italics. Lower panel: Immunocytochemistry demonstrating the expression of the epitope-tagged somatostatin $sst_{2(b)}$ receptor in CHO-K1 cells. (A) The HA antibody does not cross-react with wildtype-CHO-K1 cells. (B) In CHO-$sst_{2(b)}$ cells, strong labelling at the plasma membrane (arrowhead) as well as punctate staining over the cells is seen using the HA antibody to detect the N-terminal tag of the $sst_{2(b)}$ receptor.

maximum degree of inhibition was less marked ($-79.8 \pm 6.9\%$). (Figure 6A). Ptx pre-treatment (100 ng ml^{-1}) abolished the inhibitory response mediated by both sst_2 receptor splice variants, unmasking a stimulatory effect on adenylate cyclase activity at higher agonist concentrations (Figure 6A and B). Thus, following Ptx, SRIF (10 μM) augmented forskolin-stimulated cyclic AMP accumulation by 201 ± 3.4 and by $178 \pm 12.2\%$ in CHO-$sst_{2(a)}$ and CHO-$sst_{2(b)}$-expressing cells, respectively. In CHO-$sst_{2(a)}$ cells, the pEC_{50} for this effect was 7.45 ± 0.09 ($n=3$), but since no clear maxima could be achieved in CHO-$sst_{2(b)}$ cells, a similar pEC_{50} value for SRIF-promoted adenylate cyclase activity could not be estimated (Figure 6B).

The effects of SRIF were also studied in cells which had been pre-treated with 10 nM SRIF for 1 h. Following SRIF pre-treatment, basal cyclic AMP were: 4.48 ± 2.14 ($n=4$) and 0.96 ± 0.24 nmoles ($n=4$), for $sst_{2(a)}$ cells and $sst_{2(b)}$ cells, respectively. In Ptx-pretreated cells, the respective values were 1.12 ± 0.53 nmoles ($n=4$) and 0.76 ± 0.45 nmoles cyclic AMP ($n=4$). The effect of forskolin (10 μM) on cyclic AMP levels were variable after cells had been pre-exposed to SRIF, causing a 2–40 fold increase in the levels of cyclic AMP.

Following SRIF pre-treatment, concentration-effect curves to SRIF in both CHO-$sst_{2(a)}$ and CHO-$sst_{2(b)}$-expressing cells were displaced to the right compared with untreated cells with no difference in the maxima. Following SRIF pre-treatment, SRIF maximally reduced forskolin (10 μM)-stimulated cyclic AMP production by $89.2 \pm 3.4\%$ (pIC_{50}: 8.27 ± 0.4; $n=3$) in CHO-$sst_{2(a)}$-cells and by $77.3 \pm 12.3\%$ (pIC_{50}: 8.46 ± 0.23; $n=5$) in CHO-$sst_{2(b)}$ cells. In Ptx-pretreated cell lines there was also a rightward displacement of the stimulatory effect of SRIF in the $sst_{2(a)}$-cells with no clear difference in the maximum response. In CHO-$sst_{2(b)}$-cells there appeared to be some reduction in the response to 10 μM SRIF (Figure 6A and B).

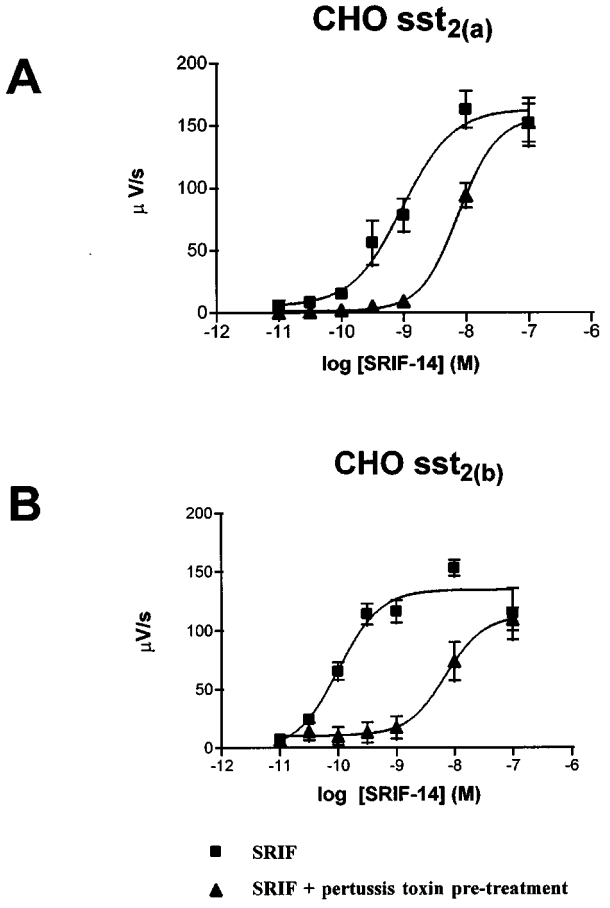

Figure 4 SRIF-induced increases in extracellular acidification rates in CHO-$sst_{2(a)}$ (A) and CHO-$sst_{2(b)}$ (B) cells in untreated cells, and following Ptx-treatment for 18 h. Data shown are the mean ± s.e.mean of three to eight different experiments and responses are given as μV/s rate change over basal.

Discussion

Molecular cloning and distribution

Using an RT-PCR based approach, we have provided the first evidence that $sst_{2(b)}$ receptor mRNA exists in the rat. The sequence of the DNA fragment isolated from rat gastric mucosa shows sequence identity in the overlap region with the previously published rat sst_2 sequence (Kluxen *et al*., 1992), indicating that the mRNA for the $sst_{2(b)}$ receptor is indeed generated by alternative splicing from a cryptic splice site as suggested by Patel *et al*. (1993). A single guanosine addition was present in our sequence within the 3′ untranslated region. The significance of this addition is unclear, but may represent a polymorphism between animal strains. The translated amino acid primary structure of the carboxy-terminus shows only 73% homology to its mouse equivalent (Vanetti *et al*., 1992), an interesting finding with regard to the very high sequence homology of the rat and mouse $sst_{2(a)}$ receptor. This may explain the operational differences observed between the mouse and the rat $sst_{2(b)}$ receptor, notably with respect to the desensitization characteristics (see below).

In order to study and compare the functional characteristics of the rat $sst_{2(b)}$ with that of the rat $sst_{2(a)}$ receptor, both receptors were expressed in CHO-K1 cells and their effects on agonist-induced stimulation of EAR and inhibition of adenylate cyclase were studied. In this recombinant system, we have shown that both somatostatin $sst_{2(a)}$ and $sst_{2(b)}$ receptors can couple efficiently to at least two effector systems. Initially, we used microphysiometry, a technique that measures extracellular acidification rates and which has previously been successfully used to functionally characterize G-protein coupled recombinant receptors (Castro *et al*., 1996; Garnovskaya *et al*., 1997) to examine the operational characteristics of both receptor types. In both cell lines, SRIF potently and concentration-dependently increased extracellular acidification rates, but SRIF was approximately ten times more potent in CHO-$sst_{2(b)}$ cells than in CHO-$sst_{2(a)}$ cells. The differences observed could not be accounted for by different receptor densities since B_{max} values for both cell lines were similar. It seems that the $sst_{2(b)}$ receptor is more efficiently coupled to induce EAR increases. In both cell lines, Ptx treatment caused a complete loss of EAR increases at low agonist concentrations. Somewhat surprisingly, however, higher concentrations of agonist resulted in EAR increases with maxima similar to those of the untreated cells, which was manifested as a rightward shift of the concentration-effect curve. This suggests that Ptx-sensitive as well as -insensitive G proteins were involved in the responses produced by somatostatin in both cell lines. Following Ptx treatment, sensitivity to SRIF was nearly identical in both cell lines indicating that the ability to couple to non Gi/Go proteins is very similar for both receptor isoforms.

During the course of our experiments we observed an apparent desensitization effect in both $sst_{2(a)}$ and $sst_{2(b)}$ receptor-expressing cells, which was evident at high agonist concentrations. To investigate this effect, responses to two single maximal SRIF concentrations, given with a 60 min

interval apart, were measured. It was found that untreated cells showed marked desensitisation whilst Ptx-treated cells exhibited less marked desensitization. We suggest that in both cell lines the effects mediated by Ptx-sensitive G proteins have a higher propensity to desensitise, compared with those mediated by non Gi/Go proteins. A number of different mechanisms might be involved including differential receptor phosphorylation by G protein receptor kinases (GRK), receptor internalization or even differential association with RGS (regulators of G protein coupling) proteins (Druey *et al*., 1996).

The effects of SRIF on forskolin-stimulated adenylate cyclase activity was also examined. Low concentrations of SRIF inhibited forskolin-stimulated cyclic AMP formation in both somatostatin $sst_{2(a)}$ and $sst_{2(b)}$ receptor expressing cell lines. The finding that both receptor splice variants couple to adenylate cyclase is in contradistinction to a previous study characterizing the mouse $sst_{2(a)}$ and $sst_{2(a)}$ receptor variants, where the $sst_{2(a)}$ receptor failed to inhibit adenylate cyclase activity, although the $sst_{2(b)}$ receptor did cause inhibition of forskolin-stimulated cyclic AMP production (Reisine *et al*., 1993). It is possible that the apparent differences between the

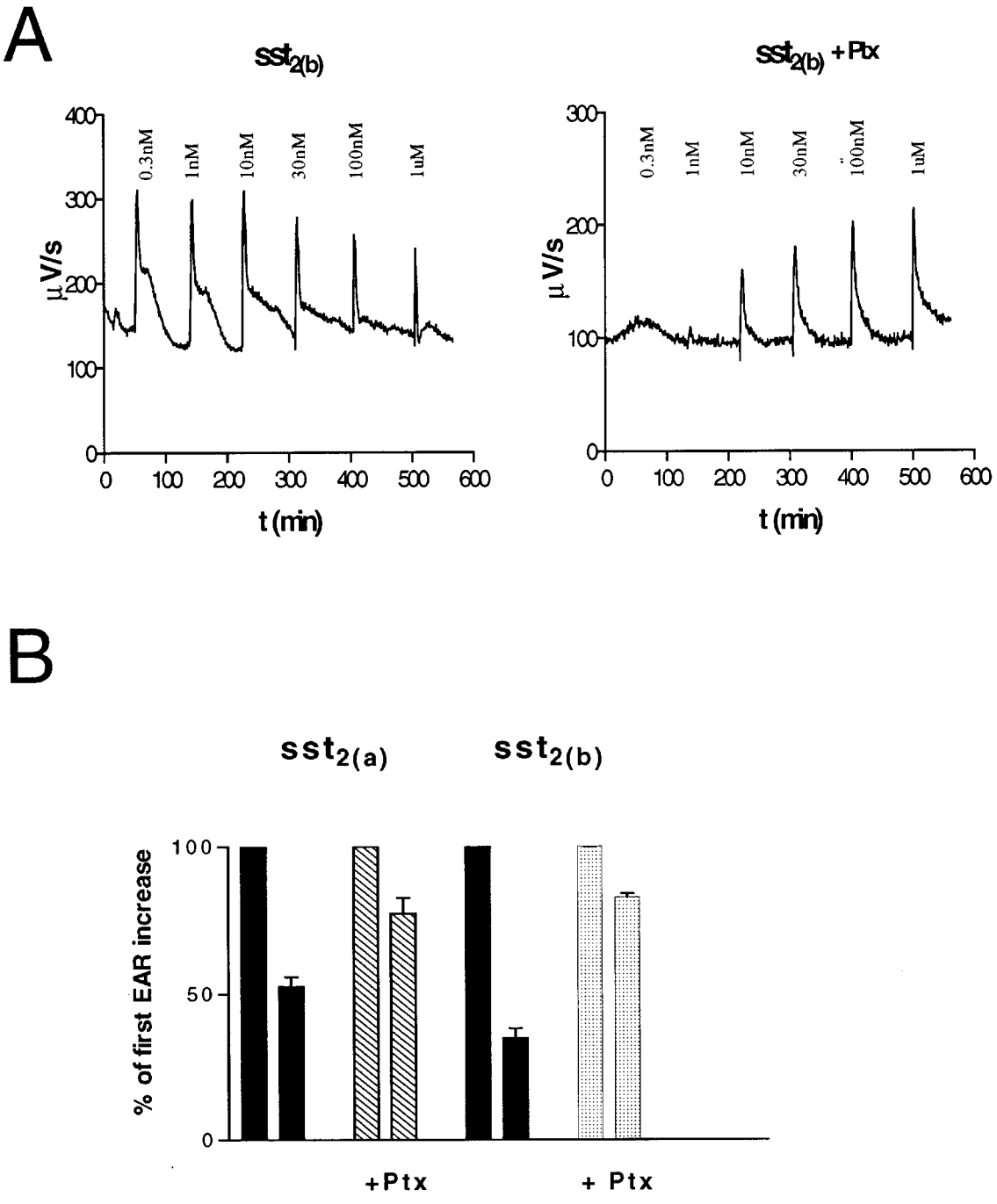

Figure 5 (A) Cytosensor recordings showing increases in extracellular acidification rates in response to SRIF-14 concentrations in CHO-$sst_{2(b)}$ cells and following pertussis toxin (Ptx)-treatment (100 ng.ml^{-1}). Note the apparent desensitisation after higher agonist concentrations in untreated cells. (B) Desensitization experiment. Two maximal (1 μM) concentrations of SRIF-14 were applied with a 60 min interval between and EARs were measured after both agonist challenges. Data are expressed as the percentage of the EAR increase to the first agonist concentration; this response was set to 100%. Data are the mean $\pm$ s.e.mean of three to five different experiments carried out in duplicate.

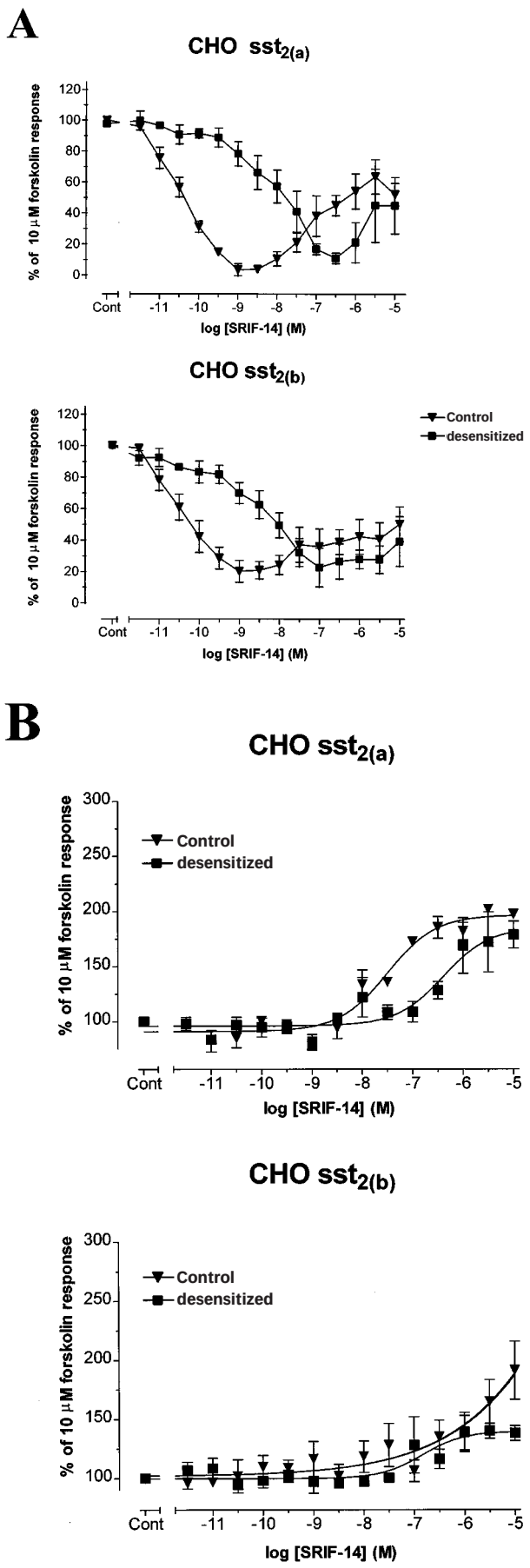

Figure 6 (A) Control cells: SRIF-induced inhibition of forskolin-stimulated cyclic AMP production in untreated (▼), and SRIF (10 nM) pretreated (■) CHO-K1 cells. (B) Ptx-treated cells SRIF-induced stimulation of adenylate cyclase in untreated (▼), and pretreated (■) CHO-K1 cells. Data are the mean ± s.e.mean of three to six different experiments.

rat and mouse receptor isoforms may partly be caused by a different cellular background, i.e. COS-7 vs CHO-K1 cells. It seems unlikely that the aminoterminal epitope tag present on the rat somatostatin $sst_{2(a)}$ and $sst_{2(b)}$ receptors is responsible for these differences, since epitope tags are not believed to alter the pharmacology of heptahelical receptors in general or somatostatin receptors in particular (von Zastrow & Kobilka, 1992; K. Smalley, W. Feniuk, J. Koenig, A. Warner, unpublished data).

The observed inverted bell-shaped concentration-effect curve seen in the present study with both receptor variants after higher agonist concentrations, may suggest the involvement of non-Gi-like proteins. This is further corroborated by the finding that Ptx treatment abolished the inhibition of adenylate cyclase in both cell lines but a stimulatory component was retained. This was internally consistent with the microphysiometry data, where we observed a stimulation of EAR after high somatostatin concentrations in Ptx-treated cells, indicating that in both assays $sst_{2(a)}$ and $sst_{2(b)}$ receptors can couple to either Gi/o or both Gi and possibly Gs, depending on the agonist concentration. Agonist-induced activation of a single receptor resulting in signalling *via* multiple classes of G-proteins has been described for a number of G-protein linked receptor systems (Milligan, 1993). In the adenylate cyclase assay, pre-exposure of the cells to SRIF caused an apparent desensitization to subsequent concentrations of SRIF, shifting the concentration-effect curve to the right along the concentration axis, although similar maxima were obtained in both the $sst_{2(a)}$ and $sst_{2(b)}$ receptor lines. Hence, both cell lines are prone to receptor desensitization, which, under the conditions used in this study, increased the pEC_{50} values by about 100 fold. Similar rightward displacements of concentration-effect curves for the adenylate cyclase inhibition assay after acute agonist pre-exposure have also been observed for other G_i/G_0-coupled receptors. Such effects for the α_{2A}-adrenoceptor in Chinese hamster fibroblasts and the adenosine A_3 receptor in CHO cells are thought to have their basis in receptor phosphorylation mediated by βARK (Ligett *et al*., 1992; Palmer *et al*., 1995). In our study, both rat $sst_{2(a)}$ and $sst_{2(b)}$ receptors desensitized, unlike the mouse homologues. This is an interesting difference between species and on the basis of these data it may be possible to identify the protein locus or even single amino acid residues responsible for desensitization potentially initiated by phosphorylation and/or internalization.

In conclusion, the results from the present study demonstrate the effective coupling of both the rat recombinant $sst_{2(a)}$ and $sst_{2(b)}$ receptors to different transduction pathways dependent upon agonist concentrations. Both receptors appear to couple similarly to Gi/o as well as to other G proteins. These observations presumably have implications for the study of somatostatin receptor-G protein coupling where single concentrations of agonist may be studied, for example co-immunoprecipitations (Law *et al*., 1993; Gu *et al*., 1995), since the composition of the receptor-G protein complex will depend on the concentration of the agonist. The differences between the operational characteristics of the rat recombinant receptor isoforms studied here are small and, if anything, the reverse of those reported for the mouse $sst_{2(a)}$ and $sst_{2(b)}$ receptors (Reisine *et al*., 1993; Vanetti *et al*., 1993). Our finding that both splice variants activate similar secondary messenger

pathways to a similar degree in a common host cell line may be surprising, but the subtle differences observed may be much more marked in a different cellular background or on other intracellular pathways. Indeed, recent preliminary data, indicate that the rat $sst_{2(a)}$ and the $sst_{2(b)}$ receptor may mediate opposing effects on cellular proliferation in CHO-K1 cells, with the former inhibiting and the latter promoting cell growth (F. Alderton, unpublished data). These data, together with the recently demonstrated different distribution of the two receptor isoforms in the rat gastric mucosa using immunohistochemistry (Kidd *et al*., 1998), may point to distinct physiological roles for both splice variants.

References

BROWN, B.L., ALBANO, J.D., EKINS, R.P. & SGHERZI, A.M. (1971). A simple and sensitive saturation assay method for the measurement of adenosine 3′ : 5′-cyclic monophosphate. *Biochem. J.,* **121,** 561 – 562.

CASTRO, S.W., FENIUK, W. & HUMPHREY, P.P.A. (1996). Differences in the operational characteristics of the human recombinant somatostatin receptor types, sst1 and sst2, in mouse fibroblast (Ltk-) cells. *Br. J. Pharmacol.,* **117,** 639 – 646.

CHOMCZYNSKI, P. & SACCHI, N. (1987). Single-step method of RNA isolation by acid guanidinium thiocyanate-phenol-chloroform extraction. *Anal. Biochem.,* **162,** 156 – 159.

DORNAUD, P., GU, Y.Z., SCHONNBRUNN, A., MAZELLA, J., TANNENBAUM, G.S. & BEAUDET, A. (1996). Localization of the somatostatin receptor sst2A in rat brain using a specific anti-peptide antibody. *J. Neurosci.,* **16,** 4468 – 4478.

DRUEY, K.M., BLUMER, K.J., KANG, V.H. & KEHRL, J.H. (1996). Inhibition of G-protein-mediated MAP kinase activation by a new mammalian gene family. *Nature,* **379,** 742 – 746.

EPELBAUM, J. (1986). Somatostatin in the central nervous system: physiology and pathological modifications. *Prog. Neurobiol.,* **27,** 63 – 100.

GARNOVSKAYA, M.N., GETTYS, T.W., VAN BIESEN, T., PRPIC, V., CHUPRUN, J.K. & RAYMOND, J.R. (1997). 5-HT_{1A} receptor activates Na^+H^+ exchange in CHO-K1 cells through $G_{1\alpha2}$ and $G_{1\alpha3}$. *J. Biol. Chem.,* **272,** 7770 – 7776.

GU, W.Z., BROWN, P.J., LOOSE-MITCHELL, D.S., STORK, P.J.S. & SCHONBRUNN, A. (1995). Development and use of a receptor antibody to characterize the interaction between somatostatin receptor subtype 1 and G proteins. *Mol. Pharmacol.,* **48,** 1004 – 1014.

HOYER, D., BELL, G.I., BERELOWITZ, M., EPELBAUM, J., FENIUK, W., HUMPHREY, P.P.A., O'CARROLL, A-M., PATEL, Y.C., SCHONBRUNN, A., TAYLOR, J.E. & REISINE, T. (1995). Classification and nomenclature of somatostatin receptors. *Trends Pharmacol. Sci.,* **16,** 86 – 88.

HUNYADY, B., HIPKIN, R.W., SCHONBRUNN, A. & MEZEY, E. (1997). Immunohistochemical localization of somatostatin receptor sst2A in the rat pancreas. *Endocrinology,* **138,** 2632 – 2635.

KIDD, E.J., SCHINDLER, M., WYATT, M.A., SELLERS, L.A. & HUMPHREY, P.P.A. (1998). Molecular cloning, expression and localisation of the rat somatostatin $sst_{2(b)}$ receptor splice variant in the rat gastric mucosa. *Br. J. Pharmacol.,* **123,** 125P.

KLUXEN, F-W., BRUNS, C. & LÜBBERT, H. (1992). Expression cloning of a rat brain somatostatin receptor cDNA. *Proc. Natl. Acad. Sci. (U.S.A.),* **89,** 4618 – 4622.

LAW, S.F., YASUDA, K., BELL, G.I. & REISINE, T. (1993). $G_{i\alpha3}$ and $G_{(o)\alpha}$ selectively associate with the cloned somatostatin receptor subtype SSTR2. *J. Biol. Chem.,* **268,** 587 – 590.

LIGGETT, S.B., OSTROWSKI, J., CHESNUT, L.C., KUROSE, H., RAYMOND, J.R., CARON, M.G. & LEFKOWITZ, R.J. (1992). Sites in the third intracellular loop of the alpha 2A-adrenergic receptor confer short term agonist-promoted desensitization. Evidence for a receptor kinase-mediated mechanism *J. Biol. Chem.,* **267,** 4740 – 4746.

LLOYD, K.C.K., WANG, J., AURANG, K., GRONHED, P., COY, D.H. & WALSH, J.H. (1995). Activation of somatostatin receptor subtype 2 inhibits acid secretion in rats. *Am. J. Physiol.,* **268,** G102 – 108.

MILLIGAN, G. (1993). Mechanisms of multifunctional signalling by G protein-linked receptors. *Trends Pharmacol. Sci.,* **14,** 239 – 244.

PALMER, T.M., BENOVIC, J.L. & STILES, G.L. (1995). Agonist-dependent phosphorylation and desensitization of the rat A3 adenosine receptor. Evidence for a G-protein-coupled receptor kinase-mediated mechanism. *J. Biol. Chem.,* **270,** 29607 – 29613.

PATEL, Y.C., GREENWOOD, M., KENT, G., PANETTA, R. & SRIKANT, C.B. (1993). Multiple gene transcripts of the somatostatin receptor SSTR2: tissue selective distribution and cAMP regulation. *Biochem. Biophys. Res. Comm.,* **192,** 288 – 294.

REISINE, T. & BELL, G.I. (1995). Molecular properties of somatostatin receptors. *Neuroscience,* **67,** 777 – 790.

REISINE, T., KONG, H.Y., RAYNOR, K., YANO, H., TAKEDA, J., YASUDA, K. & BELL, G.I. (1993). Splice variant of the somatostatin receptor 2 subtype, somatostatin receptor 2B, couples to adenylyl cyclase. *Mol. Pharmacol.,* **44,** 1008 – 1015.

SAMBROOK, J., FRITSCH, E.F. & MANIATIS, T. (1989). *Molecular cloning – a laboratory manual, Cold Spring Harbor Laboratory Press, New York, U.S.A.*

SANGER, F., NIKLEN, S. & SOULSON, A.R. (1977). DNA sequencing with chain-terminating inhibitors. *Proc. Natl. Acad. Sci. (U.S.A.),* **74,** 5463 – 5467.

SCHINDLER, M., HUMPHREY, P.P.A. & EMSON, P.C. (1996). Somatostatin receptors in the central nervous system. *Progr. Neurobiol.,* **50,** 9 – 47.

SCHINDLER, M., SELLERS, L.A., HUMPHREY, P.P.A. & EMSON, P.C. (1997). Immunohistochemical localisation of the somatostatin $sst_{2(a)}$ receptor in rat brain and spinal cord. *Neuroscience,* **76,** 225 – 240.

SCHINDLER, M., CARRUTHERS, A.M., FENIUK, W. & HUMPHREY, P.P.A. (1998). Somatostatin-induced increases in extracellular acidification rates, activation of MAP-kinase and inhibition of adenylyl cyclase in CHO-K1 cells expressing rat sst_{2A} and sst_{2B} receptors. *Br. J. Pharmacol.,* **123,** 110P.

VANETTI, M., KOUBA, M., VOGT, G. & HÖLLT, V. (1992). Cloning and expression of a novel mouse somatostatin receptor (SSTR2B). *FEBS Lett.,* **311,** 290 – 294.

VANETTI, M., VOGT, G. & HÖLLT, V. (1993). The two isoforms of the mouse somatostatin receptor (mSSTR2A and mSSTR2B) differ in coupling efficiency to adenylate cyclase and in agonist-induced desensitisation. *FEBS Lett.,* **331,** 260 – 266.

VANETTI, M., ZIÓLKOWSKA, B., WANG, X., HORN, G. & HÖLLT, V. (1994). mRNA distribution of two isoforms of somatostatin receptor 2 (mSSTR2A and mSSTR2B) in mouse brain. *Mol. Brain Res.,* **27,** 45 – 50.

VON ZASTROW, M. & KOBILKA, B.K. (1992). Ligand-regulated internalization and recycling of human beta 2-adrenergic receptors between the plasma membrane and endosomes containing transferrin receptors. *J. Biol. Chem.,* **267,** 3530 – 3538.

WYATT, M., FENIUK, W. & HUMPHREY, P.P.A. (1996). Somatostatin sst_2 receptor-mediated inhibition of parietal cell function in rat isolated gastric mucosa. *Br. J. Pharmacol.,* **119,** 905 – 910.

(Received April 15, 1998
Revised June 15, 1998
Accepted June 17, 1998)